JOURNAL OF MATERIALS SCIENCE 24 (1989) 4458–4466

Mechanical properties of Co_3Ti polycrystals alloyed with various additions

Y. LIU, T. TAKASUGI, O. IZUMI, H. SUENAGA
Institute for Materials Research, Tohoku Unversity, Sendai 980, Japan

Third elements including vanadium, tantalum, chromium, molybdenum, tungsten, iron, nickel, aluminium and germanium, were added to $L1_2$-type Co_3Ti polycrystals with a composition of 23 at% Ti. Tensile tests from 77 to 1273 K were carried out to investigate the mechanical properties of these alloys. Anomalous increases of the yield stress with increasing temperature were observed from 473 to 973 K (or 1100 K depending on the strain rates) for all tested alloys. It was also observed that the yield stress increased with decreasing temperature below 473 K and decreased with increasing temperature above 973 K (or 1100 K). The yield stresses above the peak temperature were very sensitive to the strain rate and grain size. Microstructural observation showed that grain-boundary sliding had a considerable contribution to the fall in yield stress at high temperatures. The elongation showed a maximum around 673 K and a minimum around 1073 K for all alloys. Microstructural and fractographic observation showed that most alloys tested suffered from hydrogen-related embrittlement at ambient temperatures and grain-boundary cavitation-related embrittlement around 1073 K. Addition of aluminium and iron was found to produce a significant improvement in hydrogen-related embrittlement at room temperature.

1. Introduction

Ordered alloys and intermetallic compounds have been a topic for their potential advantages over conventional, disordered alloys for high-temperature structure applications. Some of these alloys having $L1_2$ structure are particularly of interest because their yield strength shows an increase, rather than a decrease, with increasing temperature. However, the major problem in developing ordered alloys and intermetallic compounds for structural uses has been the brittleness due to grain-boundary fracture. Some efforts have been made to produce ductile ordered alloys and intermetallic compounds. For example, $L1_2$-type Ni_3Al can be made ductile by micro-alloying with boron [1] or macro-alloying with manganese or iron [2–5]. Also, Co_3V ordered alloy can be made ductile by changing the crystal structure from the brittle hexagonal structure to the higher symmetry cubic ($L1_2$) structure $(Fe, Co)_3V$ [6].

Based on electronic and structural studies on grain boundaries, it has been shown that the ductility of $L1_2$-type compounds can be manipulated by a proper selection of component elements and by an appropriate control of composition [7–11]. Based on this idea, polycrystalline Co_3Ti was found to have high grain-boundary strength and therefore to be ductile [12]. Also, increased high strength of Co_3Ti at elevated temperatures indicates that this material is a candidate for high-temperature applications. On the other hand, it has been shown that the ductility of this alloy is very sensitive to environmental conditions [13]. For example, elongation as high as 40% can be obtained when tensile tested in vacuum, but this value goes down to only a few per cent when tensile tested in air. This degradation of ductility has been suggested to be caused by hydrogen-assisted grain-boundary weakening [13]. Many mechanical properties of this alloy may be expected to be improved by the alloying method. In this paper, we report the mechanical properties of $L1_2$-type Co_3Ti polycrystals with additional elements including transition metals and B subgroup elements in the Periodic Table. The strength, ductility and fracture behaviour of these ternary Co_3Ti were characterized by tensile tests over a wide range of testing temperature. Emphasis is not placed on clarifying the mechanisms involved in many phenomena found in this work, but on understanding the alloying effect and grain-size effect (as a material factor), and the temperature dependence, environmental effect and strain-rate effect (as a testing factor). Associated detailed mechanisms will be described in different papers.

2. Experimental details

According to the site occupation and the solubility limit of third elements in Co_3Ti [14], nickel was added to substitute for cobalt, and vanadium, tantalum, chromium, molybdenum, tungsten, aluminium and germanium were added to substitute for titanium. Also, the alloy containing iron was designed to have a composition so that iron would substitute for cobalt and titanium equally. The base composition of the binary Co_3Ti was Co–23 at% Ti which is in the middle of the solid solution range of this compound (γ'). The starting materials are 99.9 wt% Co, 99.8 wt% Ti, 99.7 wt% V, 99.9 wt% Ta, 99.3 wt%

0022–2461/89 $03.00 + .12

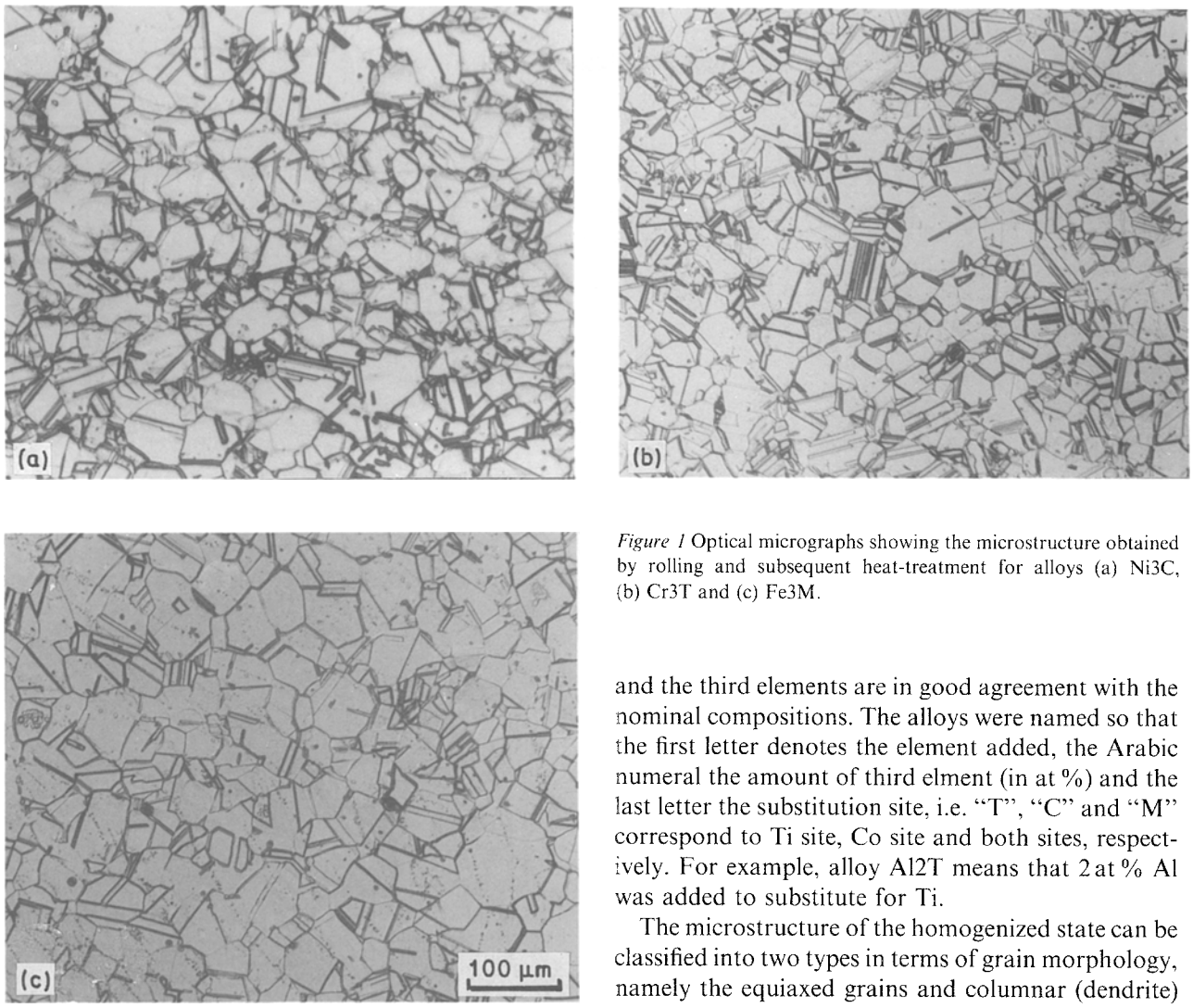

Figure 1 Optical micrographs showing the microstructure obtained by rolling and subsequent heat-treatment for alloys (a) Ni3C, (b) Cr3T and (c) Fe3M.

Cr, 99.9 wt % Mo, 99.9 wt % W, 99.9 wt % Fe, 99.9 wt % Ni, 99.99 wt % Al and 99.99 wt % Ge in purity. The alloy ingots, in the form of square rods, were produced by the arc-melting technique in an argon atmosphere. After homogenization in a vacuum of about 1.3×10^{-3} Pa at 1323 K for 2 d, the ingots were rolled to 40% reduction at 673 K in air. Tensile specimens 2 mm wide, 1 mm thick and 22 mm gauge length were prepared by wire-slitting and electro-erosion techniques. Heat treatment at 1273 K for 10 h in a vacuum degree mentioned above provided recrystallized microstructures. These specimens were then polished by finer abrading papers to remove surface damage.

Tensile tests were conducted using an Instron-type machine at a nominal strain rate of 1.1×10^{-4} sec^{-1} and 5.5×10^{-2} sec^{-1}. Tests at 77 K were carried out in liquid nitrogen. The others were conducted in a vacuum better than 1.3×10^{-3} Pa. Room-temperature tests were also conducted in air to check the environmental effect. The microstructure and fractured surface were examined by optical microscopy (OM) and scanning electron microscopy (SEM), respectively.

3. Results

3.1. Chemical composition and microstructure

Table I shows the chemical compositions of alloys used in this study. The analysed values of both titanium and the third elements are in good agreement with the nominal compositions. The alloys were named so that the first letter denotes the element added, the Arabic numeral the amount of third elment (in at %) and the last letter the substitution site, i.e. "T", "C" and "M" correspond to Ti site, Co site and both sites, respectively. For example, alloy Al2T means that 2 at % Al was added to substitute for Ti.

The microstructure of the homogenized state can be classified into two types in terms of grain morphology, namely the equiaxed grains and columnar (dendrite) grains. These depend on the phase diagram (i.e. solidification process) modified by the third elements added [15]. Equiaxed grains were formed in the alloys which contained non-equilibrium phase in the as-cast state while columnar grains were formed in alloys which showed the equilibrium phase of γ' in the as-cast state. In the equiaxed grains, homogenization produced transformation of non-equilibrium phase to γ' phase, resulting in equiaxed grains of γ'. However, recrystallization treatment produced equiaxed grains of about 30 μm in all the ternary alloys, regardless of the third elements (examples are shown in Fig. 1). Therefore, the differences in the mechanical properties obtained will be true contributions to the alloying effect, and not to the microstructural effect.

TABLE I Chemical nominal (analysed) composition (at %) of alloys used in this work

Alloys	Ti	Third element
V3T	20 (19.8)	3 (2.95)
Ta1T	22 (-)	1 (-)
Cr3T	20 (19.9)	3 (2.85)
Mo1T	22 (21.9)	1 (1.00)
W1T	22 (21.9)	1 (0.99)
Fe3M	21.5 (21.4)	3 (2.87)
Ni3C	23 (-)	3 (-)
Al2T	21 (20.9)	2 (2.07)
Ge2T	21 (20.9)	2 (2.03)

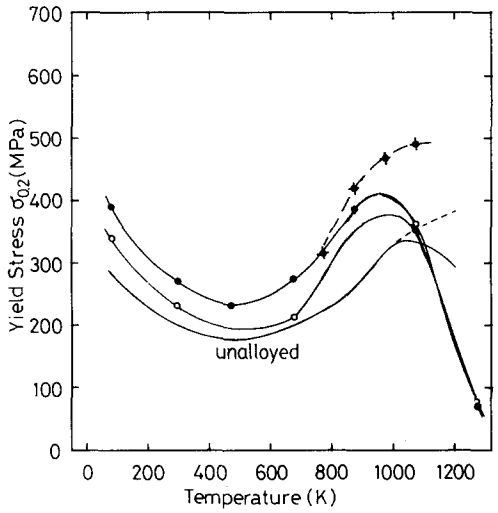

Figure 2 0.2% yield stress against temperature curves measured at two strain rates for alloys (○, ◇) V3T and (●, ◆) Ta1T, the third elements of which belong to group Va in the Periodic Table. $\dot{\varepsilon}$ = (○, ●) $1.1 \times 10^{-4}\,sec^{-1}$, (◇, ◆) $5.5 \times 10^{-2}\,sec^{-1}$.

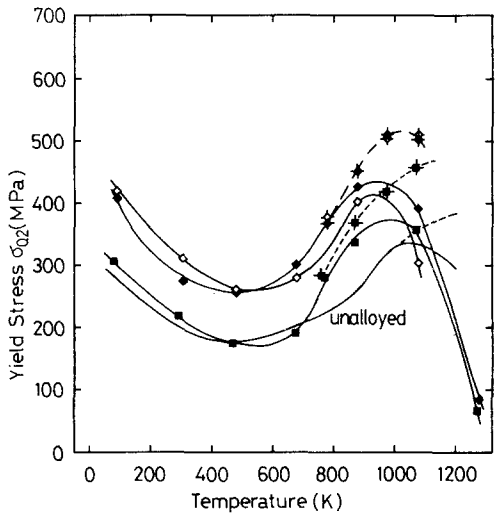

Figure 4 0.2% yield stress against temperature curves measured at two strain rates for alloys (■, ■) Fe3M, (◇, ◇) Al2T and (◆, ◆) Ge2T, the third elements of which belong to group VIII and B-subgroup in the Periodic Table, respectively. $\dot{\varepsilon}$ = (◇, ◆, ■) $1.1 \times 10^{-4}\,sec^{-1}$, (◇, ◆, ■) $5.5 \times 10^{-2}\,sec^{-1}$.

3.2. Mechanical properties

3.2.1. Temperature, strain rate and grain size dependence of the yield stress and the ultimate tensile stress

The temperature and strain-rate dependence of the yield stress for each alloy is shown in Figs 2 to 4, together with that for binary (unalloyed) Co–23 at % Ti which has similar microstructure and was tested under similar experimental conditions [13]. The curve of the yield stress against temperature for each alloy is similar. The yield stress increases with increasing temperature from 473 K to about 973 K at a strain rate of $1.1 \times 10^{-4}\,sec^{-1}$ (and a higher temperature at a strain rate of $5.5 \times 10^{-2}\,sec^{-1}$). Below 473 K, the yield stress increases with decreasing temperature. Third elements did not apparently affect the temperature (T_b) where the minimum in the yield stress appears, but slightly decreased the temperature (T_p) where the maximum of the yield stress is seen. Below T_p, higher strengthening in the yield stress is observed in most alloys. In particular, rather pronounced strengthenings are found for alloys Ta1T, W1T and alloys with B sub-group additives aluminium and germanium. Above T_p, the yield stresses in tested alloys show little difference, but rapidly decreased compared to that of binary alloys.

A positive strain-rate dependence of the yield stress was observed above 800 K for all alloys. A further investigation on the effects of strain rate and grain size was made at 1073 K for alloy Al2T and is shown in Fig. 5. Here the grain sizes were controlled by changing the annealing time. As indicated in this figure, a pronounced strain-rate dependence was recognized for the specimens with smaller grain size. At the lowest strain rate tested ($1.1 \times 10^{-4}\,sec^{-1}$), higher yield strength is obtained for larger grain size and vice versa. The reverse was true for higher strain rate ($5.5 \times 10^{-2}\,sec^{-1}$). The above phenomenon suggests that the grain-boundary sliding has played a role in lowering the yield stress in these alloys, although the yield stress of the grain interior itself (i.e. a single crystal containing no grain boundaries) showed a positive strain-rate dependence at temperatures above T_p [16]. Fig. 6 shows the optical micrograph of alloy Al2T

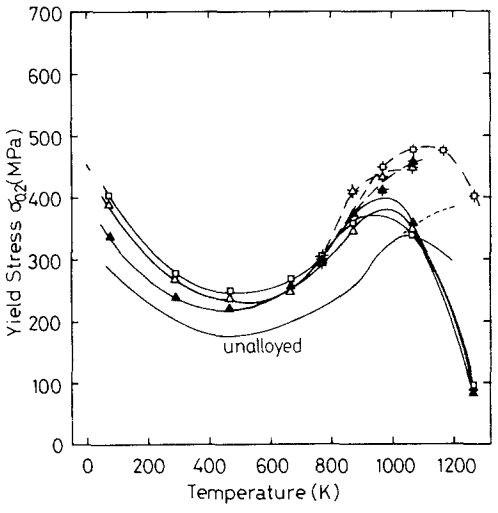

Figure 3 0.2% yield stress against temperature curves measured at two strain rates for alloys (△, ▲) Cr3T, (▲, ▲) Mo1T and (□, □) W1T, the third elements of which belong to group VIa in the Periodic Table. $\dot{\varepsilon}$ = (△, ▲, □) $1.1 \times 10^{-4}\,sec^{-1}$, (△, ▲, □) $5.5 \times 10^{-2}\,sec^{-1}$.

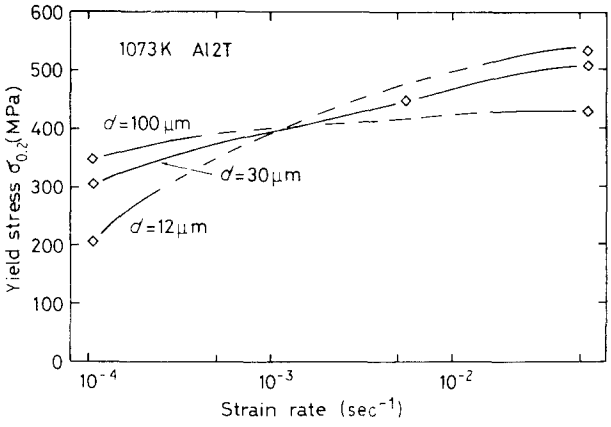

Figure 5 The effects of strain rate and grain size on the 0.2% yield stress for alloy Al2T tensile tested at 1073 K.

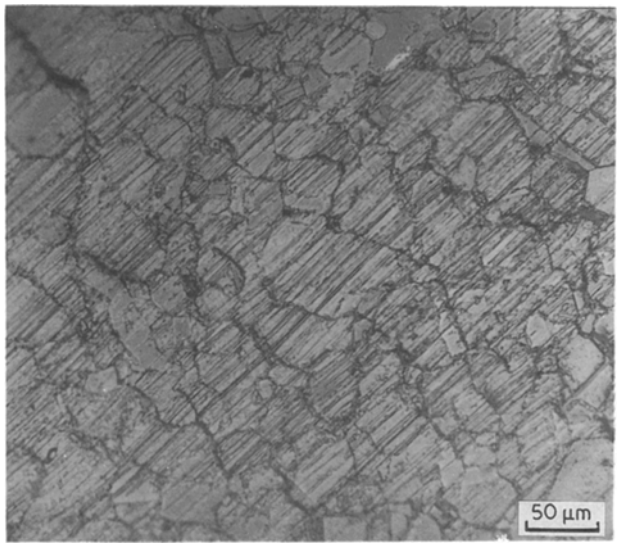

Figure 6 Optical observation of the grain-boundary sliding of alloy Al2T tested at 1073 K.

which was tensile tested at 1073 K to an elongation of 0.2% plastic strain. It is clearly seen that some scratched straight lines marked before deformation have been broken at grain boundaries, thus suggesting the occurrence of grain-boundary sliding.

A basically negative temperature dependence of the ultimate tensile strength (UTS) was observed for each alloy as shown in Figs 7 to 9, together with that for unalloyed Co–23 at % Ti. Typical examples are alloys Fe3M and Al2T, the UTS of which decreases monotonically with increasing temperature. However, at low temperatures of 77 and 298 K, a fall in UTS to a greater or lesser extent occurred for the other alloys. Alloys Mo1T and Ge2T showed smaller values at 77 K and at room temperature than at 473 K. This trend for the UTS–temperature curve is identical to the elongation behaviour described later.

The effects of strain rate and grain size on the UTS of alloy Al2T were examined at 1073 K and are shown

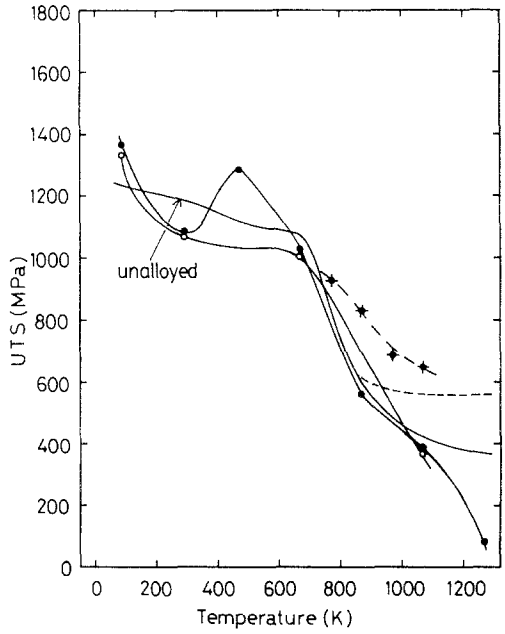

Figure 7 Ultimate tensile strength (UTS) against temperature curves tested at two strain rates for alloys (○, ◇) V3T and (●, ◆) Ta1T. $\dot{\varepsilon}$ = (○, ●) 1.1 × 10^{-4} sec^{-1}, (◇, ◆) 5.5 × 10^{-2} sec^{-1}.

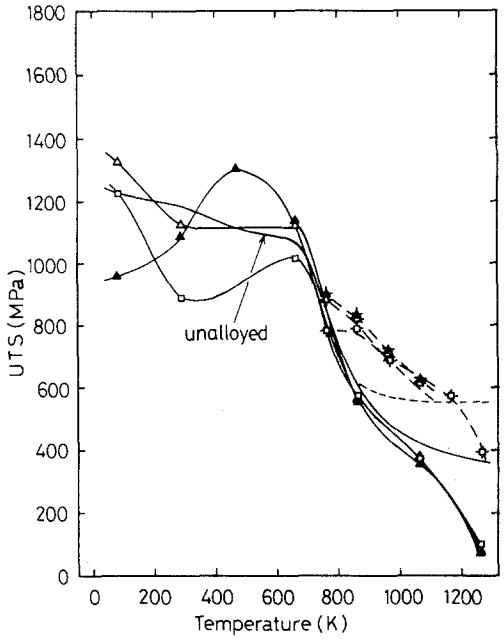

Figure 8 Ultimate tensile strength (UTS) against temperature curves tested at two strain rates for alloys (△, ◇) Cr3T, (▲, ◆) Mo1T and (□, ◇) W1T. $\dot{\varepsilon}$ = (△, ▲, □) 1.1 × 10^{-4} sec^{-1}, (◇, ◆, ◇) 5.5 × 10^{-2} sec^{-1}.

in Fig. 10. The pronounced positive strain-rate dependence of the UTS was again observed. The specimen with smaller grain size showed sharper change in the UTS with strain rate. The variation in the UTS with grain size is relatively large at low strain rates while it is small at high strain rates.

3.2.2. Temperature, strain rate and grain-size dependence of elongation

Figs 11 to 13 show the elongation of each alloy as a function of temperature from 77 to 1273 K for two strain rates, 1.1 × 10^{-4} sec^{-1} and 5.5 × 10^{-2} sec^{-1}. Here, the elongation values obtained in binary

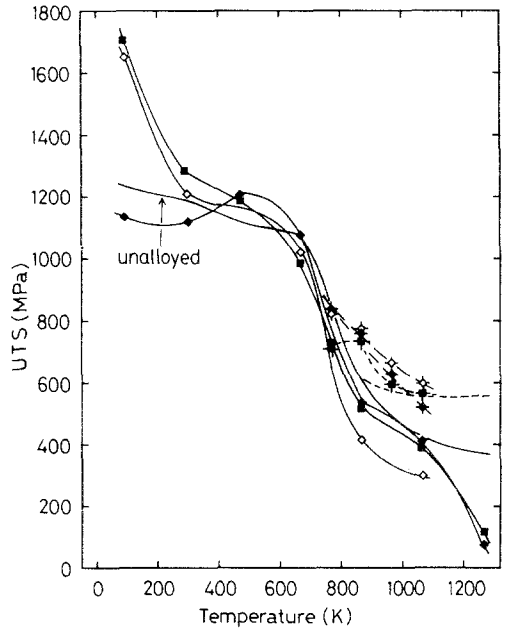

Figure 9 Ultimate tensile strength (UTS) against temperature curves tested at two strain rates for alloys (■, ◆) Fe3M, (◇, ◇) Al2T and (◆, ◆) Ge2T. $\dot{\varepsilon}$ = (◇, ◆, ■) 1.1 × 10^{-4} sec^{-1}, (◇, ◆, ■) 5.5 × 10^{-2} sec^{-1}.

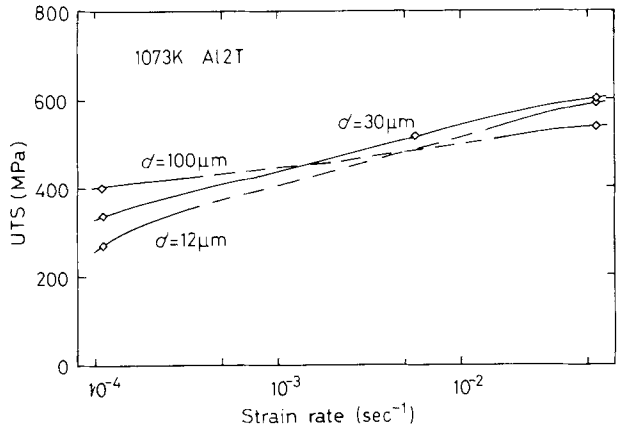

Figure 10 The effects of strain rate and grain size on the UTS for alloy Al2T tensile tested at 1073 K.

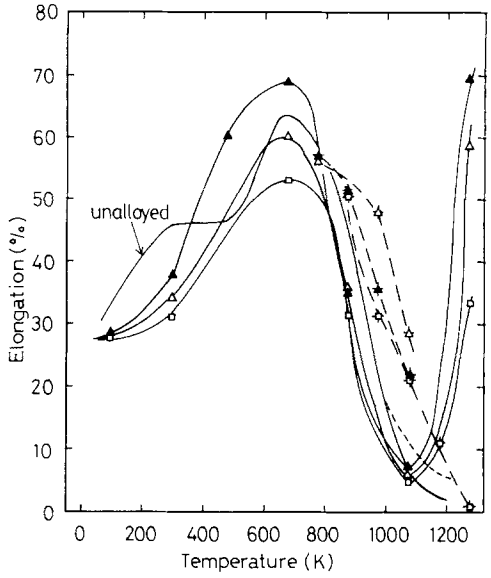

Figure 12 Elongation against temperature curves tested at two strain rates for alloys (△, ☆) Cr3T, (▲, ★) Mo1T and (□, ✠) W1T. $\dot{\varepsilon}$ = (△, ▲, □) 1.1 × 10^{-4} sec^{-1}, (☆, ★, ✠) 5.5 × 10^{-2} sec^{-1}.

Co–23 at % Ti were again included for the comparison. First, it is noticed that high elongations are available over a wide range of temperature for all alloys and also the curves of elongation against temperature are basically similar to those of the UTS against temperature. A significant alloying effect on elongation was observed, particularly, at 77 and 298 K. Alloys Fe3M and Al2T showed the largest elongation of 83% and 66% at 77 K, respectively, while for most alloys elongation was reduced at these temperatures. The effect of alloying element on this phenomenon will be discussed later from the viewpoint of hydrogen embrittlement. Also, the elongation showed a minimum around 1073 K and then rapidly increased at sufficiently high temperatures (i.e. above 1073 K) for all alloys tested at a strain rate of 1.1 × 10^{-4} sec^{-1}.

This elongation behaviour can be well rationalized by fractography. Macroscopically, the fracture surfaces of the specimens deformed below 773 K were inclined at about 45° to the tensile axis, corresponding approximately to the plane of maximum shear stress. Microscopic observation of a fracture surface by SEM indicated that the transgranular fractures are dominant (see Fig. 14). Above 773 K, the macroscopic fracture surfaces tended to take their directions perpendicular to the tensile axis. Microscopically, the fracture surface changed from dimple form to intergranular form with a certain deformation feature. Fracture in this temperature region is considered to be controlled by the formation and coalescence of voids (cavities) at grain boundaries. At 1273 K, as seen in Fig. 14, the fracture surface consists of smaller "coral" patterns which indicate evidence of migration of grain boundaries. Thus, the high elongation obtained in this temperature is due to the dynamic recrystallization, resulting in accommodation of stress concentration formed at prior grain boundaries. The evidence for this is also shown in Fig. 15. The optical micrograph taken after 50% plastic deformation at 673 K indicates

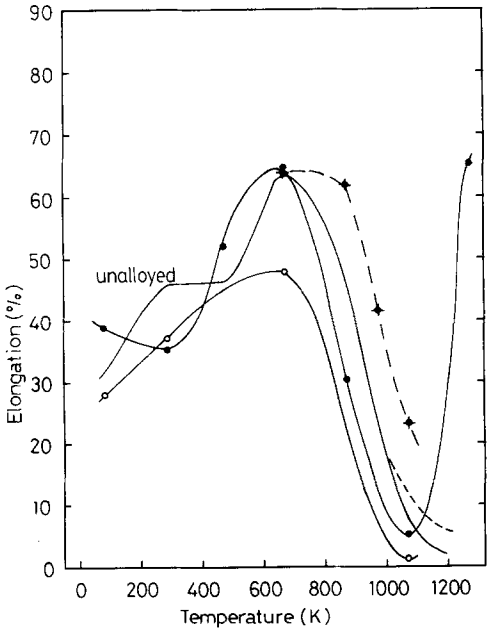

Figure 11 Elongation against temperature curves tested at two strain rates for alloys (○, ◇) V3T and (●, ◆) Ta1T. $\dot{\varepsilon}$ = (○, ●) 1.1 × 10^{-4} sec^{-1}, (◇, ◆) 5.5 × 10^{-2} sec^{-1}.

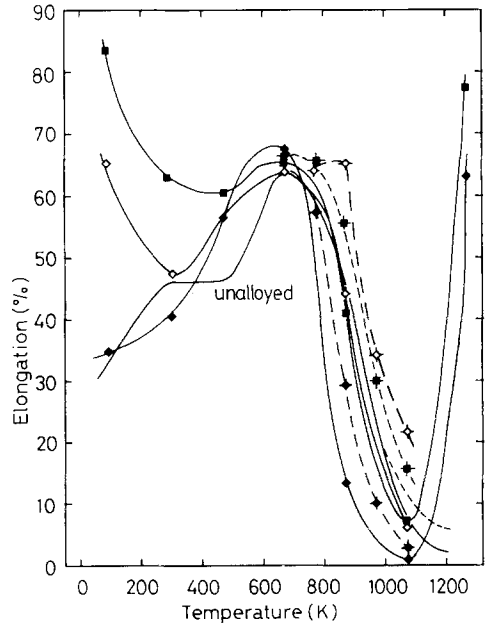

Figure 13 Elongation against temperature curves tested at two strain rates for alloys (■, ▣) Fe3M, (◇, ◈) Al2T and (◆, ◈) Ge2T. $\dot{\varepsilon}$ = (◇, ◆, ■) 1.1 × 10^{-4} sec^{-1}, (◈, ◈, ▣) 5.5 × 10^{-2} sec^{-1}.

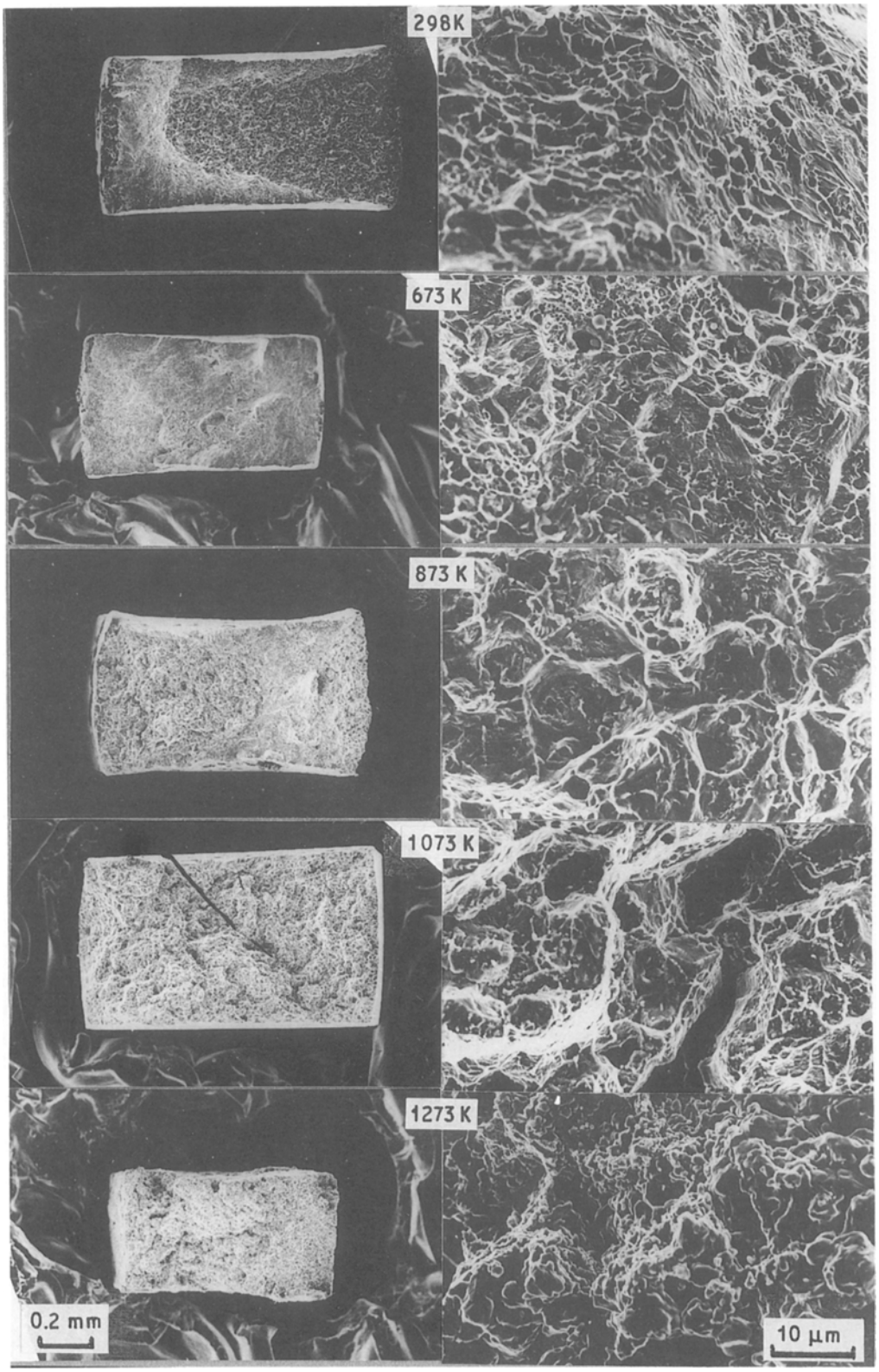

Figure 14 Fractographs taken from alloy Cr3T tested at various temperatures at a strain rate of 1.1×10^{-4} sec^{-1}. Note that tensile axis is horizontal in these photographs.

that the grains have been elongated along the tensile axis, thus indicating deformation by dislocation gliding. This feature, however, is not observed on the sample deformed to about 30% elongation at 1273 K. Instead, many small grains were observed to nucleate at original grain boundaries, suggesting that they were formed during deformation.

Higher elongations were obtained at temperatures from 773 to 1073 K when alloys were tested at higher strain rates of 5.5×10^{-2} sec^{-2}. In addition, the elongation minimum, which is postulated to be accomplished by the competition of the two diffusion-controlled processes, i.e. the grain-boundary cavitation and dynamic recrystallization, tended to shift to the higher temperature region at a higher strain rate.

The strain rate and grain-size dependence of elongation for alloy Al2T were examined at 1073 K and are shown in Fig. 16. A positive strain-rate dependence was observed on this property. At low strain rates, the specimen with the smaller grain size

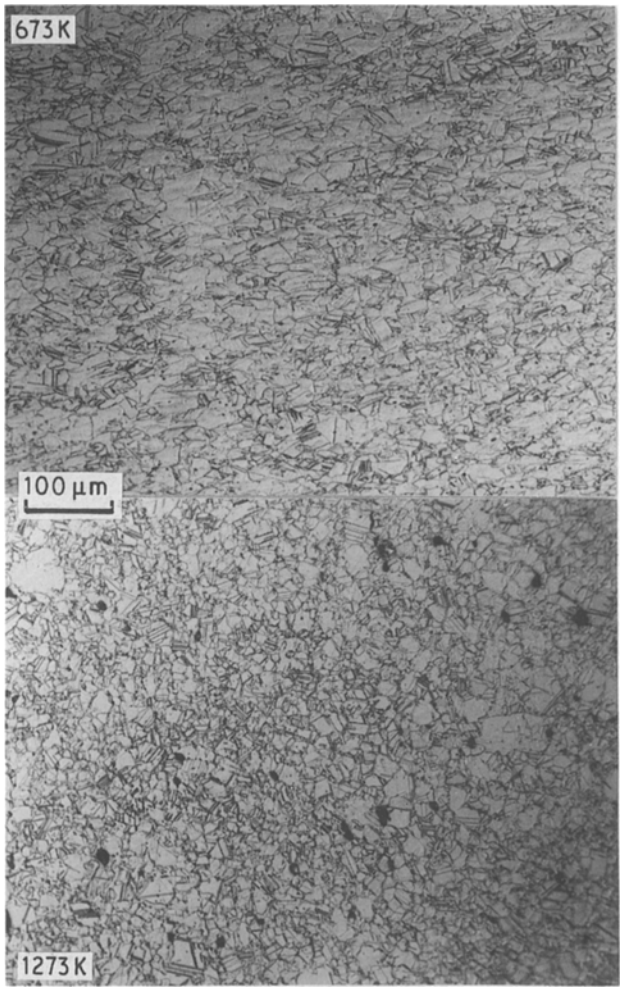

Figure 15 Optical micrographs taken from alloy W1T tested at 673 and 1273 K.

showed a larger elongation. At high strain rates, larger elongation was obtained for the specimens with intermediate grain size, i.e. 30 μm.

3.2.3. Environmental effect on the mechanical properties

As mentioned above, remarkable reductions in elongation and UTS were observed at 77 and 298 K for most alloys. This degradation became severer when these alloys were tested in air. Fig. 17 compares the elongations of the samples tensile tested in air with those in a vacuum better than 1.3×10^{-3} Pa. Both tests were performed at room temperature at a strain

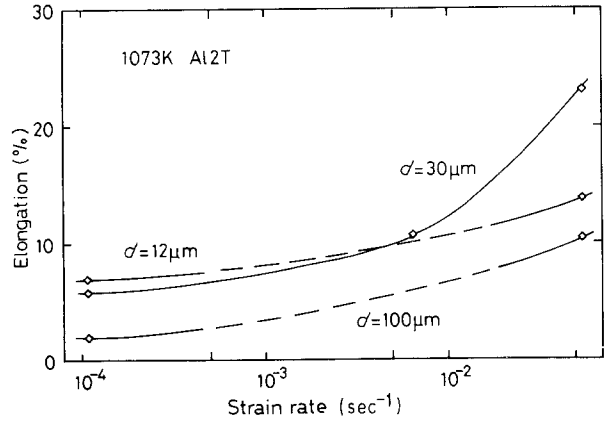

Figure 16 The effects of strain rate and grain size on elongation for alloy Al2T tensile tested at 1073 K.

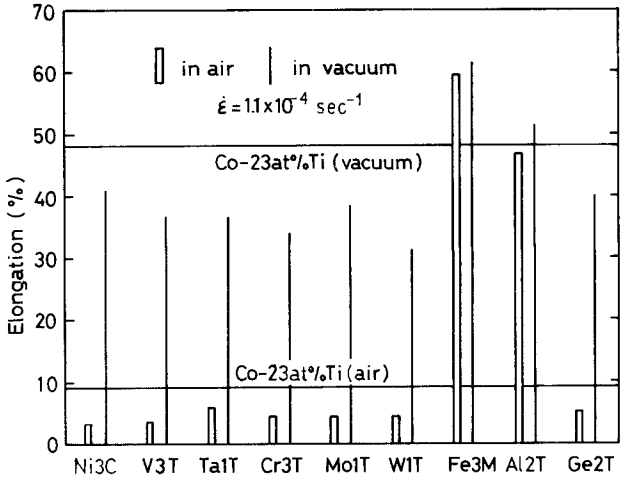

Figure 17 A comparison of the air tested and vacuum tested elongation for each alloy.

rate of 1.1×10^{-4} sec^{-1}. There are almost one order differences in elongation between air-tested samples and vacuum-tested samples for most alloys. Therefore, it is suggested that the marked elongation loss seen at 77 and 273 K (see Figs 11 to 13) can be correlated with the elongation degradation occurring in air. In other words, these two phenomena are controlled by the same mechanism. Here, it is interesting that for alloys Fe3M and Al2T relatively high values of elongation and UTS were obtained in both environmental conditions and their differences were very small. Thus, it is suggested that iron and aluminium are the effective elements in reducing the degradation of the mechanical properties mentioned above.

Fracture surfaces examined by SEM indicate that there is a good correlation between fractography and elongation. A vacuum-tested sample exhibited an almost transgranular fracture surface with a dimple pattern. The fracture surface of the air-tested sample is composed mostly of an intergranular fracture pattern with grain boundary facets (see Fig. 18). Optical examination on the fractured side surface showed that most of the cracks nucleated at the sample surface and then propagated into the sample interior along grain boundaries.

4. Discussion

The deformation mechanism of Co_3Ti compound has been investigated using binary Co_3Ti [16] and $(Co \cdot 3\,at\,\%\ Ni)_3Ti$ single crystals [17]. The sharp increase in the yield stress with decreasing temperature below room temperature was suggested to be due to the non-planar core of the superlattice intrinsic stacking fault (SISF) dissociated superdislocation [18]. Macromeasurement on orientation dependence of the critical resolved shear stress (CRSS) and microobservation on the dislocation structure strongly suggest that the Kear–Wilsdorf cross-slip mechanism [19] is operating at elevated temperatures in this material. Also, it has been shown that the reduction of the yield stress at further high temperatures is due to the operation of {0 0 1} slips instead of {1 1 1} slips. It was thus concluded that the yield property of Co_3Ti intermetallic compounds is attributed to the unique structure of the dislocation core.

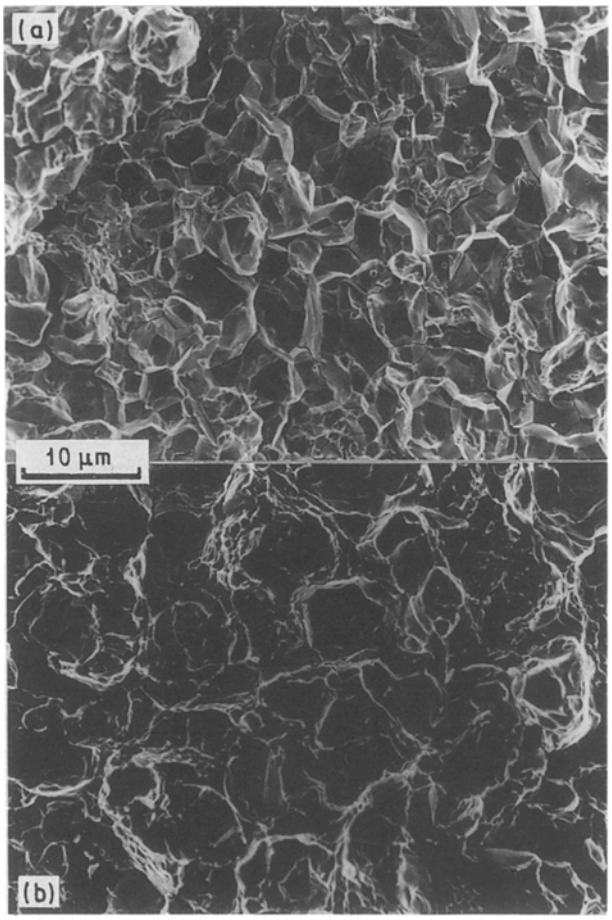

Figure 18 Opti al observation of the fractured surface of alloy W1T tested in (a) air and (b) vacuum.

First, we consider the effect of the third elements on the yield strength. It has been proposed that the CRSS for (1 1 1) [$\bar{1}$ 0 1] slip can be expressed as

$$\tau = \tau_G + \tau_n + \tau_p$$

where τ_G is the shear stress required to move a straight superdislocation with a planar core, τ_n the increase of the CRSS below T_b, and τ_p the increase of the CRSS above T_b [17]. Here, it is postulated that τ_G depends only on the temperature change of the shear modulus, and therefore is almost constant, while τ_n and τ_p are thermal stress components operating at temperatures below and above T_b, respectively.

The effect of the third elements could be evaluated from the changes in each stress component. First, τ_G reflects the solution hardening due to the third elements. τ_G could be estimated here by the yield stress at 473 K where the contribution due to the two thermally activated processes, i.e. τ_n and τ_p, is postulated to be small. The results obtained here indicated that the third elements tantalum, tungsten, aluminium and germanium showed a relatively high yield stress around T_b, indicating larger solution hardening effects. In order to evaluate more quantitatively this athermal stress, we tried to correlate the yield stress observed at 473 K with atomic size parameter determined from the lattice parameter change [14], or with the shear modulus parameter or with their combined parameter. However, the result indicated good correlation with neither of these. This may reveal that the yield stress at 473 K still involves the stress contributions of τ_n and τ_p. Indeed, the analysis for single crystals showed that the yield stress at T_b consists of these three stress components [17]. Next, the effect of third elements on τ_n could be evaluated by whether or not they stabilize the SISF dissociated superdislocation core, or whether they promote a core transition from the SISF dissociation to the APB dissociation [17]. Finally, the effect of the third elements on τ_p could be predicted by their effects on the cross-slip behaviour from the (1 1 1) plane to the (0 1 0) plane. For example, in order to evaluate the alloying effect on this process, the activation energy was estimated from the stress increase $\Delta\tau$, which were defined as the stress difference between the testing temperature and 473 K, with reciprocal temperature. However, the alloying effect on this parameter was ambiguous. This may be due to the fact that the amount of third elements added to Co_3Ti was small in the present case, and to the fact that the polycrystals used modified the intrinsic alloying effect on the yield stress at temperatures above T_b through easy operation of grain-boundary sliding.

Another important point is the intrinsically high (cohesive) strength of grain boundaries of Co_3Ti, unlike Ni_3Al. A recent study on the grain-boundary features in $L1_2$ structures showed that the grain-boundary strength fundamentally depends on the heterogeneity of the bondings between two like atoms and two unlike atoms [7–9]. A compound composed of two metal elements with similar electro-chemical nature is expected to have less heteropolarity in electron distribution in the grain boundary, resulting in enhanced grain-boundary strength.

For the alloying effect on the elongation at ambient temperatures, where the ductility is assumed to be controlled directly by the grain-boundary cohesive strength, the obtained results are consistent with the above model [7–9]. Alloys with the addition of B-subgroup element (Ge2T) and some other transition metals (Ta1T, Mo1T, and W1T) substituting for the titanium site showed lower values of elongation, relative to that of binary (unalloyed) Co_3Ti. This trend is predicted by the criterion based on the valency difference between the third element and the constitutive solvent element substituted. That is, the valency differences are negative for these alloys. On the other hand, alloy Fe3M with iron substituting for half the titanium sites and alloy Al2T with aluminium substituting for the titanium sites showed higher or almost the same values, relative to that of unalloyed Co_3Ti. In these two alloys, the valency differences are positive or almost zero.

A remarkable environmental effect on the mechanical properties was observed in ternary Co_3Ti alloys tested at ambient temperatures. It has been suggested that this effect is associated with hydrogen embrittlement [13]. Hydrogen penetrating from the air influenced especially the elongation and the UTS of these materials, through promoting grain-boundary fracture [13]. In the alloying effect on the hydrogen-related elongation reduction, the alloys with added iron and aluminium showed the most resistive behaviour.

Extensive work is being carried out to reach an explicit understanding of this [20] because this alloying effect is very important from the viewpoint of materials development of Co_3Ti compounds. Details of the micromechanism associated with this alloying effect will be reported in a subsequent paper.

The elongations at elevated temperatures are controlled by two diffusion mechanisms, i.e. and cavitation at grain boundaries and dynamic recrystallization, and therefore are very sensitive to strain rate. The former was dominant at lower temperatures. Thus, the minimum in elongation is the result of the competition between the two diffusion-controlled processes. As the strain rate increases, it is expected that the cavitations at grain boundaries will occur effectively at higher temperatures and thereby the intergranular fracture will appear at higher temperatures; at the same time, the dynamic recrystallization is operative at higher temperatures. Consequently, the minimum in elongation shifted to higher temperatures when the specimens were tested at a higher strain rate. The alloying effect on elongation, then, must appear through changing the diffusion constant (diffusivity) of the alloy. It is noticed among a number of added elements that alloy W1T showed the lowest value of elongation at 1273 K, suggesting a stronger resistance to recrystallization and grain growth. Also, the trend is quite identical to the alloying effect on the "static" recrystallization and grain growth [21]. Thus, it is suggested that the elements with higher melting points could lower the diffusivity of the components in Co_3Ti, and thereby affect the elongation at high temperatures.

5. Conclusions

The mechanical properties of Co_3Ti polycrystals alloyed with various third elements were investigated at temperatures from 77 to 1273 K and the following results were obtained.

1. All of the alloys tested showed that the variation of yield stress with temperature was characterized by the T_b (referred to as the bottom temperature at 473 K) and T_p (referred to as the peak temperature at 973 or 1100 K), similar to that of binary Co_3Ti. The yield stresses around and above T_p were very sensitive to the strain rate and grain size, and were considerably lowered by the onset of grain-boundary sliding. Also, a significant strengthening effect at temperatures below T_p were observed for alloys with additions of tantalum, tungsten, aluminium and germanium.

2. The variation of elongation with temperature for most alloys was characterized by the maximum at 673 K and the minimum around 1073 K. Around room temperature, the ducilities of most alloys were reduced by air testing compared with vacuum testing. This behaviour was attributed to the hydrogen embrittlement characterized by intergranular fracture. The additives iron and aluminium showed the most resistive nature to this embrittlement. At the minimum temperature in elongation, all the alloys suffered from severe grain-boundary cavitation. At sufficiently higher temperatures, dynamic recrystallization occurred and resulted in the recovery of elongation. A strong sensitivity of elongation to strain rate and grain size was observed at high temperature.

Acknowledgement

This research was partly supported by Grant-in-Aid for Scientific Research on Priority Area, New Functionality Materials-Design, Preparation and Control, The Ministry of Education, Science and Culture.

References

1. K. AOKI and O. IZUMI, *Nippon Kinzoku Gakkaishi* **43** (1979) 1190.
2. T. TAKASUGI, O. IZUMI and N. MASAHASHI, *Acta Metall.* **33** (1985) 1259.
3. N. MASAHASHI, T. TAKASUGI and O. IZUMI, *J. Mater. Sci.* **22** (1987) 2599.
4. *Idem, Metall. Trans.* **19A** (1988) 345.
5. J. A. HORTON, C. T. LIU and M. L. SANTELLA, *ibid.* **18A** (1987) 1265.
6. C. T. LIU, *Int. Metals Rev.* **29** (1984) 168.
7. T. TAKASUGI and O. IZUMI, *Acta Metall.* **31** (1983) 1187.
8. *Idem, ibid.* **33** (1985) 1247.
9. T. TAKASUGI, O. IZUMI and N. MASAHASHI, *ibid.* **33** (1985) 1259.
10. *Idem, ibid.* **35** (1987) 381.
11. O. IZUMI and T. TAKASUGI, in "High-Temperature Ordered Intermetallic Alloys II", edited by N. S. Stoloff, C. C. Koch, C. T. Liu and O. Izumi, MRS Symposium, Vol. 81 (1987) p. 173.
12. T. TAKASUGI and O. IZUMI, *Acta Metall.* **33** (1985) 39.
13. *Idem, ibid.* **34** (1986) 607.
14. Y. LIU, T. TAKASUGI and O. IZUMI, *Met. Trans.* **17A** (1986) 1433.
15. Y. LIU, Master dissertation, Tohoku University (1985).
16. T. TAKASUGI, S. HIRAKAWA, O. IZUMI, S. ONO and S. WATANABE, *Acta Metall.* **35** (1987) 2015.
17. Y. LIU, T. TAKASUGI, O. IZUMI and S. ONO, *Phil. Mag. A* **59** (1989) 401.
18. Y. LIU, T. TAKASUGI, O. IZUMI and T. TAKAHASHI, *ibid.* **59** (1989) 423; 454.
19. B. H. KEAR and H. G. F. WILSDORF, *Trans. AIME* **224** (1962) 382.
20. Y. LIU, T. TAKASUGI, O. IZUMI and T. YAMADA, *Acta Metall.* **37** (1989) 507.
21. Y. LIU, Doctor dissertation, Tohoku University (1988).

Received 20 September 1988
and accepted 24 February 1989